

## Interplay between the Coulomb explosion and vicinage effects studied using $H_2^+$ molecules under channeling conditions

R. C. Fadanelli, P. L. Grande, M. Behar, and J. F. Dias

*Instituto de Física Federal University of Rio Grande do Sul, Avenida Bento Gonçalves, 9500, CEP 91501-970 Porto Alegre (RS), Brazil*

K. Czerski

*Institute of Physics, University of Szczecin, Szczecin, Poland*

G. Schiwietz

*Hahn-Meitner Institut, Abteilung SF4, Glienicker Strasse 100, D-14109 Berlin, Germany*

(Received 7 December 2005; revised manuscript received 12 May 2006)

The aim of this work is to investigate how the mean energy loss and straggling due to  $H_2^+$  molecules interacting with silicon are affected by the Coulomb explosion and vicinage effects. To that end, a SIMOX-type sample made up of  $^{18}O$  and with an appropriate  $^{18}O$  marker grown over the surface of crystalline Si was employed, allowing to carry out the measurements through the  $^{18}O(p, \alpha)^{15}N$  resonant reaction at 151.2 keV under channeling and random directions. The results show that the mean energy loss associated with the Coulomb explosion and vicinage effects are similar and amount each to about 2% of the total mean energy loss. The comparison of the energy straggling obtained for molecular beams at random and the well-aligned  $\langle 100 \rangle$  direction shows a larger value for the aligned case, which is interpreted as a result of the Coulomb explosion along the channel direction. The experimental results are also discussed in terms of Monte Carlo simulations.

DOI: XXXX

PACS number(s): 68.55.Ln, 34.50.Bw, 61.85.+p, 36.40.-c

### I. INTRODUCTION

The study of the molecular stopping power is more complex than the one concerned with single ions. In fact, when  $H_2^+$  and  $H_3^+$  molecules interact with matter, additional non-trivial effects may come into play. When these molecules penetrate any material, they lose their electrons in the first atomic layers of the material. At this point, an electrostatic repulsion force acts among the components of the molecule, leading to what is known as a Coulomb explosion,<sup>1</sup> i.e., the particles move away from each other as they travel through the medium. The potential experienced by the constituents of the molecule is basically a Coulomb potential screened by the electrons of the medium and depends on the speed of the projectiles. A second effect to be considered is that as each proton of the molecule interacts nonadiabatically with the electrons of the medium, it induces a so-called wake potential which, in turn, will influence the motion of the trailing particles of the molecule. The overall interference pattern of the “dressed” excitation potential generated among the molecular constituents is termed a vicinage effect, which leads to the well-known fact that the energy loss of molecules differs from the sum of the energy losses of each individual particle.<sup>2</sup> A clear manifestation of this effect can be seen, for instance, in the results obtained in a previous work<sup>3</sup> and, more recently, for the energy loss of  $H_3^+$  ions in  $SiO_2$  films.<sup>4</sup>

When a molecule travels along a major axial direction in a crystal, i.e., under channeling conditions, the Coulomb explosion will provide an extra transversal energy to the individual atoms of the molecule. Consequently, these atoms tend to approach closer to the channel walls, thus enhancing the energy transfer to the medium. This process, referred to as transverse Coulomb heating energy, was initially studied

using either the transmission<sup>5</sup> or the backscattering<sup>6</sup> techniques. Although these experiments established the basis for further studies, they provided limited information on the fundamental processes at play. More recently, new backscattering results interpreted in terms of computer simulations allowed a better understanding of the consequences due to the Coulomb explosion of molecules under channeling conditions.<sup>7</sup> Moreover, a refined experiment combining the detection of both x-rays and backscattered particles from crystal Si allowed a quantitative measure of the transversal Coulomb heating energy.<sup>8</sup> These results showed that this energy, for the cases of  $H_2^+$  and  $H_3^+$  traveling along the  $Si\langle 100 \rangle$  channel at 150 keV/amu, amounts to  $2.6 \pm 0.6$  eV and  $5.1 \pm 0.8$  eV, respectively, which are compatible with the potential energy stored per particle in the molecule. Furthermore, it has been shown that the contribution of the transversal heating energy to the total stopping power of  $H_3^+$  molecules in the  $Si\langle 100 \rangle$  direction amounts to about 5%.<sup>9</sup>

Despite all the improvements achieved in theory and experiment, some challenging questions still remain open. One of them is to which extent the Coulomb explosion and the vicinage effect compete and, consequently, what are the relative contributions of these effects to the stopping power of molecules like  $H_2^+$  in crystalline Si. In order to get a detailed insight of this problem, we embarked on a new experiment employing the nuclear reaction analysis (NRA) technique. The experimental procedure, the data analysis and the results, which are interpreted in terms of simulations, are discussed in the following sections.

### II. EXPERIMENTAL PROCEDURE

In order to perform the present experiment, we have used an  $^{18}O$ -enriched SIMOX target, which is composed of a

160 nm Si(100) layer grown on top of a 400 nm Si<sup>18</sup>O<sub>2</sub> film built in a Si(100) wafer. Finally, the sample was oxidized with <sup>18</sup>O in order to obtain a very thin film (less than 1.5 nm thick) of Si<sup>18</sup>O<sub>2</sub> to act as a surface marker.

We have used the <sup>18</sup>O(*p*, α)<sup>15</sup>N resonant nuclear reaction at 151.2 keV in order to determine the energy position of the Si/Si<sup>18</sup>O<sub>2</sub> interface. Since the width of this resonance is only 50 eV, we could achieve an energy resolution of about 100 eV at the region of interest. The alpha particles resulting from the nuclear reaction were detected by a large area (600 mm<sup>2</sup>) surface-barrier detector.

Beams of H<sup>+</sup> ions and H<sub>2</sub><sup>+</sup> molecules were provided by the 500 kV ion implanter of the Physics Institute at the Federal University of Rio Grande do Sul. The samples were mounted on a three-axes goniometer and aligned along the Si(100) direction following standard procedure.<sup>8</sup> For each projectile we have taken two spectra: one under channeling condition and another in a random direction. H<sup>+</sup> and H<sub>2</sub><sup>+</sup> spectra were taken at the same energy per mass unit (about 150 keV/amu) and particle current. Moreover, all of the experiments were carried out in a chamber with a vacuum better than 10<sup>-7</sup> mbar. Finally, to avoid any damage to the sample, each NRA measurement was carried out in a different hitting position of the sample. This precaution is essential as far as channeling analysis is concerned due to the risk of Si amorphization caused by high ion fluxes. A check where a second channeling spectrum was obtained in the same spot at the target was carried out from time to time and no significant differences were found. Although the constraint concerning Si amorphization is far less severe at random direction measurements (with random meaning throughout this work a 5° tilt from the <100> channel, 30° azimuth with respect to the {100} plane), the same checking procedure described above was adopted for this case as well. Again, no significant changes were ever observed.

Figure 1 shows a typical excitation curve of the Si/Si<sup>18</sup>O<sub>2</sub> interface when H<sup>+</sup> (top panel) and H<sub>2</sub><sup>+</sup> (bottom panel) ions were used as projectiles under channeling and random conditions. We also show in the inset the whole profile, including the peak due to the <sup>18</sup>O at the surface of the sample. The most interesting feature displayed in the top panel in this figure is the difference between the random and channeling cases, namely the shift of the leading edge of the buried Si<sup>18</sup>O<sub>2</sub> layer. This shift, which is due to the difference in the random and channeling stopping powers, was determined with a precision better than 100 eV through the use of the <sup>18</sup>O surface peak as a reference. Furthermore, a numerical fit function [see Eq. (5)] for the slope and position of the energy-loss distribution of the buried <sup>18</sup>O was necessary to achieve this precision. Through the derivative of the results presented in this figure, we would get the energy loss distribution in a channeling condition. Therefore, the edge of the excitation function, which is related to the maximum of the derivative, is a measure of the mean energy loss. In the bottom panel we display the same kind of spectra obtained with H<sub>2</sub><sup>+</sup> molecules instead. Again, one can observe a shift between the channel and random energy spectra due to the same reasons mentioned above.

Figure 2 shows the excitation curve for the peak markers.

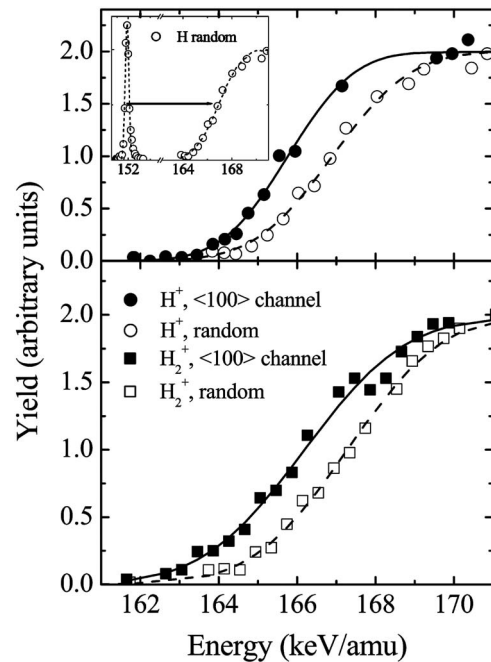


FIG. 1. Normalized excitation curves as a function of the H<sup>+</sup> (top) and H<sub>2</sub><sup>+</sup> (bottom) incident energy per proton. The inset depicts the full random spectrum featuring both the marker and the leading edge of the Si-c/SiO<sub>2</sub> interface. The curves represent the fitting results for the marker (Gaussian) and for the leading edges [Eq. (5)].

The values were renormalized in height to emphasize their relative widths. No significant peak shifts were found among these curves. However, the H<sub>2</sub><sup>+</sup> peaks (bottom panel) are broader than the H<sup>+</sup> ones (top panel) by about 300 ± 50 eV

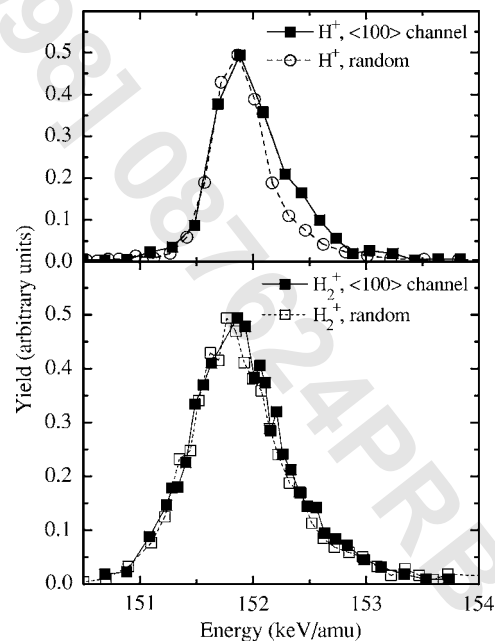


FIG. 2. Excitation curve as a function of the H<sup>+</sup> (top) and H<sub>2</sub><sup>+</sup> (bottom) and incident energy per proton for the peak markers. All peaks were normalized in height to emphasize their relative widths.

[the differences in full width at half maximum (FWHM), taken from the curves, were about 700 eV]. These differences are associated with the energy stored in the vibrational states of the molecule and, to a minor extent, to the vicinage effect on straggling. These broadenings are discussed later in this work.

### III. RESULTS AND DISCUSSION

The use of the high energy-resolution NRA technique allows the determination of the energy loss of  $H^+$  and  $H_2^+$  in Si in a straightforward manner. As a matter of fact, all fundamental processes under study in this work are connected either with the broadening of the leading edge of the Si-c/Si<sup>18</sup>O<sub>2</sub> interface, or with the differences in the relative positions of the marker (at the surface of the sample) and this edge, both under specific circumstances involving different ions ( $H^+$  or  $H_2^+$ ) and/or alignment conditions (random or channeling). Indeed, the channeling results for both  $H^+$  and  $H_2^+$  ions displayed in Fig. 1 show that the leading edges of the Si-c/Si<sup>18</sup>O<sub>2</sub> interface are always shifted toward smaller incident energies compared to the random results. This is a clear signature of the reduced energy loss under well-aligned conditions. Moreover, under channeling conditions, a substantial broadening of the Si-c/Si<sup>18</sup>O<sub>2</sub> edge is observed for the  $H_2^+$  molecules when compared with the results obtained for  $H^+$  ions, which is related to the contribution of the longitudinal Coulomb explosion with the energy straggling. In the following subsections, the results concerning the role of the Coulomb explosion on the mean energy loss and on the energy straggling will be discussed in detail.

### IV. TRANSVERSAL COULOMB EXPLOSION

In order to evaluate the energy difference  $\Delta E$  between the marker peak and the leading edge of the Si-c/Si<sup>18</sup>O<sub>2</sub> interface under different conditions, i.e.,  $H^+$  or  $H_2^+$  and channeling or random alignment, they were fitted with a Gaussian and an errorlike function, respectively. In this way, we were able to achieve the following results:

$$\Delta E_{CH+VE} = \Delta E^{chan}(H_2^+) - \Delta E^{chan}(H^+) = 540 \pm 95 \text{ eV/amu}, \quad (1)$$

$$\Delta E_{VE} = \Delta E^{ran}(H_2^+) - \Delta E^{ran}(H^+) = 300 \pm 90 \text{ eV/amu}. \quad (2)$$

In these equations, *chan* and *ran* stand for channeling and random, respectively, while CH and VE stand for Coulomb heating and vicinage effects, respectively. The uncertainties quoted in these results represent the statistical fluctuation related to the average of independent measurements. Equation (1) deals with energy differences for  $H^+$  and  $H_2^+$  ions under channeling conditions. While the concepts of Coulomb explosion and the vicinage effect do not apply for  $H^+$  ions, they are applicable for the  $H_2^+$  case. It is important to bear in mind that the Coulomb explosion changes the ion flux distribution under channeling conditions, providing an extra transversal energy to the constituents of the molecule (the

Coulomb heating energy<sup>8</sup>). Moreover, it leads mainly to a smearing out of the ion flux distribution and, consequently, the mean energy loss of  $H_2^+$  molecules under channeling but not random conditions will be influenced by this effect. Therefore, Eq. (1) represents the contribution of both Coulomb heating and vicinage effects to the energy difference  $\Delta E_{CH+VE}$ . Conversely, Eq. (2) is related to the energy difference between  $H^+$  and  $H_2^+$  ions in a random direction. Unlike the previous case, only the vicinage effect plays a role in the energy difference since the Coulomb explosion does not change the ion flux (practically uniform in this case), thus giving no extra contribution at all to the energy loss. Therefore, the energy difference  $\Delta E_{VE}$  should refer to the vicinage effect only. Assuming that the vicinage effect is the same for both random and channeling conditions (see Ref. 10), the subtraction of Eq. (2) from Eq. (1) should yield the Coulomb heating effect on the energy-loss only, which amounts to  $(240 \pm 130)$  eV/amu.

Since the present results were evaluated for  $H^+$  and  $H_2^+$  ions traveling along 160 nm of silicon crystal under different alignment conditions, Eqs. (1) and (2) represent average energies due to the vicinage plus Coulomb explosion effects and the pure vicinage effect, respectively. Unlike the vicinage effect, which takes place only in the first tens of nm, the effect of the Coulomb explosion persists for the whole distance traveled by the ions and thus it should be expressed in eV/Å. However, as shown recently,<sup>8</sup> the effectiveness of the Coulomb explosion shows up only after the molecule penetrates about 40 nm in silicon (corresponding to  $8 \times 10^{-15}$  s, in agreement with our current simulations), since the angular spreading manifests itself with delay and, moreover, needs further time to be converted into a new impact parameter distribution. Therefore, the corresponding changes in the ion flux will affect the mean energy loss along almost the whole channeling motion, while the redistribution due to the Coulomb explosion (the change in ion flux) comes to an end earlier. Thus, the Coulomb explosion fades away, but its effects in the mean energy loss remain during the residual channeling motion. In short, the effects due to the Coulomb explosion are present along 120 nm and not along the full thickness of 160 nm. Taking these facts into account, the average energy loss associated with the Coulomb explosion would amount to about 0.2 eV/Å.

In order to obtain a more detailed picture of the Coulomb heating effect on the energy loss, a Monte Carlo simulation was developed for both  $H^+$  and  $H_2^+$  ions channeling along the  $\langle 100 \rangle$  axial direction in silicon. In the case of  $H_2^+$  projectiles, the initial conditions such as the interatomic distance and the velocities of each fragment in the center-of-mass system should be calculated using the Franck-Condon principle. Since there are no such calculations for a Coulomb explosion inside a solid available yet, we generated classically the initial conditions of the fragments according to the microcanonical ensemble using the ground-state potential curve from Ref. 11 and the energies of the vibration modes from Refs. 2 and 12. In this procedure we assume that the electron from the impinging  $H_2^+$  molecule is suddenly removed along the first monolayers. The simulations were carried out over 160 nm, which corresponds to the thickness of the crystal employed in the experiments. The first step was to

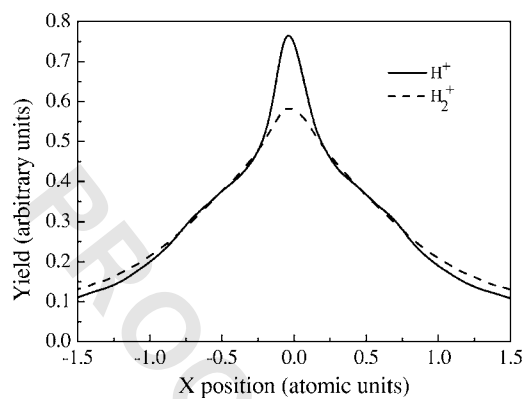


FIG. 3. Normalized averaged ion flux distribution in the Si<100> direction integrated over the  $y$  direction. The  $x$ - $y$  plane is defined by the four Si atoms perpendicular to the Si<100> direction. The channel center is taken as zero.

simulate how the ion flux in the Si<100> channel changes for the monatomic and molecular beams. To that end, Newton's equations were solved in order to describe the motion of an ensemble of ions/molecules impinging on the channel under a tilt angle  $\Psi$  (and internal angles in the case of molecules). The Molière interatomic potential was used for the interaction of the ions with the target nuclei. The angle between the molecular axis and the motion direction is chosen randomly, as well as the projectile initial position along the transverse channel plane. The interaction between the fragments of the  $H_2^+$  molecule was modeled using three different potentials: (i) a pure Coulomb potential; (ii) a Yukawa potential with a dynamic screening function according to the Arista and Lifschitz approach<sup>13</sup> (screening length of about 4 a.u. for the present case); and (iii) a wake-type potential, whose target dielectric properties were described by a Mermim dielectric function (using an electron radius of  $r_s=2$  a.u.).<sup>14</sup> Since the wake potential is noncentral, effects on the alignment of the fragments along the channel are automatically taken into account.<sup>15</sup> Therefore, the use of a wake-type potential includes both alignment and Coulomb explosion effects. These effects on the ion flux can be seen in Fig. 3, which represents the channeled ion flux, averaged along the  $z$  direction (the flight direction) and projected along the  $y$  direction, in the  $x$ - $y$  plane defined by the four central atoms around the Si<100> channel. The ion flux for the  $H^+$  beam displays the well-known flux peaking, i.e., a strong enhancement of the flux near the center of the channel. The  $H_2^+$  beam still shows the flux peaking effect. However, this effect is considerably reduced for the molecular beam due to the Coulomb explosion, which enhances the transverse energy of the molecule fragments and, consequently, produces higher ion fluxes far from the center.

A further step was taken in order to evaluate the effects of the ion flux over the mean energy loss of the molecule as a function of the tilt angle  $\Psi$  between the incoming beam and the <100> direction in Si. The unitary convolution approximation<sup>16</sup> was used in order to calculate the mean energy loss  $Q(b)$  as a function of the impact parameter  $b$ . The mean energy loss per traversed distance  $dE/dz$  as a function of  $Q(b)$  and the ion flux  $\Phi(x,y,z,\Psi)$  is then given by

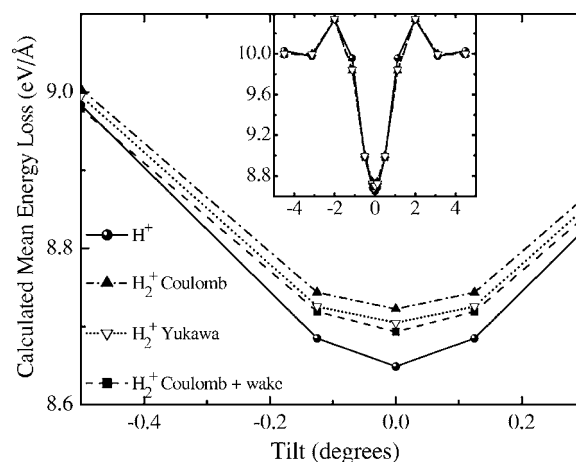


FIG. 4. Calculated mean energy loss as a function of the tilt angle around the center of the Si<100> direction. The inset depicts the full angular distribution. The interaction between the constituents of the molecule was modeled by three different potentials: pure Coulomb (full triangles connected with dot-dashed lines); wake plus Coulomb (full squares connected with dashed lines); and Yukawa (open triangles connected with dotted lines). The results for the monoatomic case are also shown (full circles connected with full lines). See the text for further information.

$$\frac{dE}{dz}(\Psi) = \frac{\int dx dy dz \Phi(x,y,z,\Psi) \bar{Q}(x,y)}{d \int dx dy dz \Phi(x,y,z,\Psi)}, \quad (3)$$

where  $d$  is the longitudinal distance among the Si atoms, and

$$\bar{Q}(x,y) = \sum_{i=1}^{N_c} Q(b_i), \quad (4)$$

where  $b_i$  represents the impact parameters relative to each atomic chain belonging to the channel and  $N_c$  is the number of atomic chains used to simulate the target. Beyond the four central atomic chains, which characterize the channel itself, another neighboring twelve chains were employed in order to ensure a proper symmetry of the potential and the mean energy loss within the central channel. The integration along the longitudinal direction ( $z$ ) is performed from the surface up to 160 nm, corresponding to the actual sample thickness of the Si layer. Finally, the integration along  $x$ - $y$  directions is performed along the transverse channel directions. Thermal vibrations as well as neutralization of the ions along their trajectories have been also included, although they contribute with less than 1% to the final mean energy loss.

The results provided by the use of Eq. (3) are shown in Fig. 4. The main feature observed in these results is that all potentials tested in the simulations provide shallower angular distributions around the center of the channel compared with the monoatomic case, which is a result of the transversal Coulomb explosion (Coulomb heating) on the channeling mean energy loss. The differences between the  $H^+$  and  $H_2^+$  results at zero degrees gives this contribution for the particular choice of potentials assumed in the calculations. This contri-

bution, along 160 nm thickness, amounts to approximately  $70\pm 5$  eV,  $88\pm 5$  eV, and  $115\pm 5$  eV under the assumptions of wake-type, Yukawa, and pure Coulomb potentials, respectively. The choice of the interparticle potential affects the importance of the quasi-Coulomb explosion on the channeling mean energy loss in two different ways. First, the energy stored in the system, which finally will be converted into kinetic energy of the fragments, is smaller for screened potentials such as the Yukawa one. Here we assume that the  $H_2^+$  molecules loose their electrons and polarize the target electrons so fast that the internuclear distance does not change very much. As a matter of fact, the time scale for screening buildup is much shorter than the molecular breakup. Second, in the case of a wake-type interaction, which is noncentral, the fragments can align along the center-of-mass velocity (even for an uniform electron gas target), turning the molecular breakup more longitudinal. Thus, both screening and noncentral interactions will reduce the value of the Coulomb heating effect.

The simulated results are smaller than the experimental ones ( $240\pm 130$  eV), especially for the case where the wake potential was employed. Only the simulation using a pure Coulomb potential lies within the experimental uncertainty limits for the contribution of the Coulomb heating. Although within two standard deviations of the confidence level for the experimental results all theoretical results agree with the experimental one, we can speculate about possible scenarios that could reduce the effect of the screening (or alignment in the case of a wake-type interaction) and thus favoring the use of a pure Coulomb potential for the breakup process under channeling conditions. Indeed, the Si valence electrons are not homogeneous as assumed in the present screened interaction (besides the first-order treatment in the case of the wake-type interaction). Since the valence electrons are localized in covalent bonds, a fraction of them are constrained to move around the channel and along the string direction. In this way, electrons should have a larger mobility along the longitudinal direction of the ion motion and around the channel because of the bounding between pairs of valence electrons, but not inside the channel where the ion is traveling. In this scenario, fewer electrons would be affected by the potential generated by the projectiles, thus leading to the effect of the screened potential between the two correlated ions. Furthermore, this would result, in the case of a wake-type interaction, in a more central net force. Although this effect may be important, its role in the present context has never been discussed so far.

Finally, effects arising from the modification of the ion-string potential due to the medium polarization have been estimated through simulations using an  $H^0$ -string potential. This may enhance the Coulomb heating effect by only about 10%. Other effects such as nonequilibrium potentials (after stripping at the surface), capture-and-loss cycles (reducing the molecular alignment), and ion beam divergence are also expected to be of minor importance.

## V. ENERGY STRAGGLING

The energy straggling for both  $H^+$  and  $H_2^+$  ions traveling under random and well-aligned conditions in the Si(100)

TABLE I. Energy straggling for  $H^+$  and  $H_2^+$  ions in Si under different alignment conditions.

Ion	Direction	Straggling $\sigma_0$ (eV)
$H^+$	Random	$1395\pm 40$
$H^+$	$\langle 100 \rangle$	$1195\pm 40$
$H_2^+$	Random	$1530\pm 70$
$H_2^+$	$\langle 100 \rangle$	$1750\pm 70$

channel can be extracted directly from the widths obtained from the fittings of the leading edge of the Si-*c*/Si<sup>18</sup>O<sub>2</sub> interface shown in Fig. 1.

Here the use of an error function to fit the widths should be avoided because the effect of the variation of energy straggling on ion penetrating distance cannot be neglected. Instead we have used the following fitting function for the nuclear reaction yield  $y(E)$  as a function of the beam energy  $E$ :

$$y(E) = N \int_0^\infty dx C(x) \exp\left(-\frac{(E - E_f - xdE/dx)^2}{2(\sigma_0^2 + \Omega_p^2 x)}\right), \quad (5)$$

where  $N$  is a normalization constant,  $C(x)$  is the O<sup>18</sup> concentration as a function of the depth  $x$  relative to the Si/SiO<sub>2</sub> interface position (a step function distribution),  $E_f$  is the resonance energy (151 keV) and  $dE/dx$  is the SiO<sub>2</sub> stopping power. Finally,  $\sigma_0$  stands for the energy straggling before the O<sup>18</sup> buried layer (which includes the energy straggling along the Si crystalline layer, the beam spreading and the kinematic transformation or Doppler effect due to the molecule vibrations),  $\Omega_p$  corresponds to the Bohr-like energy straggling per  $\text{\AA}^{1/2}$  along the SiO<sub>2</sub> matrix.

The results for  $\sigma_0$ , which represent basically the energy straggling along the Si crystalline layer, are summarized in Table I.

As expected, the results obtained for  $H^+$  ions traveling under random directions are larger than those obtained at a well-aligned direction. Conversely, the results obtained for  $H_2^+$  ions clearly point in the opposite direction, since the straggling obtained under random directions is smaller than that at a well-aligned direction. This result can be understood as an enhancement of the straggling due to the Coulomb explosion that takes place along the channeling direction, i.e., a longitudinal Coulomb explosion. Indeed, the molecular straggling  $\sigma_{H_2}$  can be understood as a quadratic combination of the atomic straggling  $\sigma_{H_1}$  with the longitudinal component of the Coulomb explosion  $\sigma_{LCE}$ . Thus using the relation

$$\sigma_{LCE} = \sqrt{\sigma_{H_2}^2 - \sigma_{H_1}^2} \quad (6)$$

we obtain  $1280\pm 110$  eV and  $625\pm 195$  eV for the longitudinal laboratory-frame component of the Coulomb explosion under channeling and random directions, respectively. In order to check these results, a simple analysis can be carried out based on the final kinetic energy  $K_H$  of each ion along the longitudinal movement:

$$K_H - K_0 = \Delta_H = U_0 \cos^2 \theta + 2 \cos \theta \sqrt{E_0 U_0}. \quad (7)$$

In this equation,  $U_0$  is the sum of the molecular potential energy (after the loss of the molecular binding electron) and the average initial kinetic energy stored per ion, in the molecule center-of-mass frame. This energy, stemming from the Coulomb explosion, would be the energy available for each proton to be converted into their kinetic energy.  $K_0$  is the initial kinetic energy of the  $\text{H}_2^+$  center of mass, and  $\theta$  is the angle between the directions of the beam and the  $\text{H}^+$  ion (in the center-of-mass frame), which is related to the Coulomb explosion. Under the assumption of an isotropic explosion, the angular average of  $\Delta_H$  in Eq. (7) is just  $U_0/3$ , which is negligible compared to  $K_0$ . Therefore, the Coulomb explosion does not affect the mean kinetic energy or the energy difference between the marker and the leading edge of the Si-*c*/Si<sup>18</sup>O<sub>2</sub> interface. However, the variance of  $\Delta_H$  is given as

$$V_{\Delta_H-r} = \sqrt{\langle \Delta_H^2 \rangle - \langle \Delta_H \rangle^2} \approx \frac{2\sqrt{3}}{3} \sqrt{K_0 U_0}. \quad (8)$$

In fact, as discussed above, the value of the stored energy  $U_0$  per fragment depends on the choice of the interatomic interaction. For the potential energy contribution, it is 3.2 eV and 5.8 eV for the Yukawa and Coulomb interaction, respectively. For the vibrational energy contribution, we performed an average of the vibrational energy distribution for  $\text{H}_2^+$  in the center-of-mass frame (see details in Refs. 2 and 12). This calculation yielded 0.5674 eV and corresponds to 337 eV in the laboratory system, which is in good agreement with the value found by analyzing the peak markers (Fig. 2), i.e.,  $300 \pm 50$  eV. The straggling component arising from the vicinage effect is less than 130 eV along the crystalline layer, assuming a broad vicinage energy loss distribution (FWHM of about 300 eV). Therefore, given our experimental uncertainties, it can be neglected in our evaluations. In this way, Eq. (8) gives a value of 831 and 1004 eV for an isotropic explosion assuming Yukawa and Coulomb potentials, respectively. A comparison of these results with the one obtained from Eq. (6) for random conditions ( $625 \pm 195$  eV) shows that the one provided by the Yukawa-type interaction is compatible with the experimental result.

For the well-aligned condition, the assumption of an isotropic explosion is no longer applicable. For this case, we have obtained the straggling due to Coulomb explosion directly from the Monte Carlo simulations. The results obtained in such way amount to  $910 \pm 20$  eV,  $1110 \pm 12$  eV and  $1169 \pm 10$  eV for Yukawa, Wake, and Coulomb interatomic potentials, respectively. Only the results obtained with a pure Coulomb interaction are in good agreement with the experi-

mental one ( $1280 \pm 110$  eV). Here, the use of the Yukawa interaction (with screening length given by Ref. 13) yields much smaller values. This result is consistent with the one observed for the transversal Coulomb explosion. The polarization provided by the Yukawa-type interaction seems to be too large for well-aligned molecules in crystal Si. It is important to stress that other choices of screening functions from Ref. 13 like, for instance, the single-zeta type, could enlarge the mean energy loss straggling due to the Coulomb explosion and the Coulomb heating effect value as well.

## VI. CONCLUDING REMARKS

A clear separation of the average energy-losses associated to the vicinage effect and the Coulomb explosion could be achieved. The results obtained in this work, namely  $300 \pm 90$  eV and  $240 \pm 130$  eV for the vicinage and the Coulomb explosion effects, respectively, along 160 nm, are similar to each other. Since the mean energy loss of  $\text{H}_2^+$  ions in the Si(100) direction at 150 keV/amu is about 14.8 keV (Ref. 9) the relative contribution of both effects to the mean energy loss at a well-aligned direction is practically the same (for this thickness), amounting each to 2% approximately. However, for thicker substrates, the effect of Coulomb heating (about 0.2 eV/Å) should prevail. This result of the Coulomb heating energy is also consistent with those obtained from a completely different experimental approach.<sup>9</sup>

Concerning the energy straggling, we have clearly observed the influence of the longitudinal component of the Coulomb explosion for  $\text{H}_2^+$  molecules under channeling and random conditions. In particular, the energy straggling for channeling  $\text{H}_2^+$  molecules is much larger than the one obtained for random conditions. This effect can be understood if we take into account that the channeling process modifies the angular distribution of the Coulomb explosion, leading to an enhanced longitudinal motion.

Monte Carlo simulations using standard screened interactions do not reproduce (within one standard deviation) our observations for the effect of the Coulomb explosion on the mean energy loss and energy straggling under channeling conditions. Only the Coulomb potential provided a good agreement for the transversal and longitudinal explosion under channeling conditions. This result indicates the need of a more realistic interatomic potential specifically designed for channeling conditions.

## ACKNOWLEDGMENTS

The authors are indebted to the Brazilian agencies CAPES (PROBRAL 166/04), CNPq, and FAPERGS as well as to DAAD (PROBRAL, Germany) for the partial support of this work.

- <sup>1</sup>D. S. Gemmell, J. Remillieux, J. C. Poizat, M. J. Gaillard, R. E. Holland, and Z. Vager, *Phys. Rev. Lett.* **34**, 1420 (1975).
- <sup>2</sup>W. Brandt, A. Ratkowski, and R. H. Ritchie, *Phys. Rev. Lett.* **33**, 1325 (1974).
- <sup>3</sup>R. Levi-Setti, K. Lam, and T. R. Fox, *Nucl. Instrum. Methods Phys. Res.* **194**, 281 (1982).
- <sup>4</sup>M. Behar, J. F. Dias, P. L. Grande, and J. H. R. dos Santos, *Phys. Rev. A* **64**, 022904 (2001).
- <sup>5</sup>J. C. Poizat and J. Remillieux, *J. Phys. B* **5**, L94 (1972).
- <sup>6</sup>J. M. Caywood, T. A. Tombrello, and T. A. Weaver, *Phys. Lett.* **37A**, 350 (1971); T. A. Tombrello and J. M. Caywood, *Phys. Rev. B* **8**, 3065 (1973).
- <sup>7</sup>V. A. Khodyrev, V. S. Kulikauskas, and C. Yang, *Nucl. Instrum. Methods Phys. Res. B* **195**, 259 (2002).
- <sup>8</sup>R. C. Fadanelli, P. L. Grande, M. Behar, J. F. Dias, G. Schiwietz, and C. D. Denton, *Phys. Rev. B* **69**, 212104 (2004).
- <sup>9</sup>R. C. Fadanelli, P. L. Grande, M. Behar, J. F. Dias, and G. Schiwietz, *Nucl. Instrum. Methods Phys. Res. B* **230**, 96 (2005).
- <sup>10</sup>N. R. Arista, *Nucl. Instrum. Methods Phys. Res. B* **164**, 108 (2000).
- <sup>11</sup>J. C. Slater, *Theory of Molecules and Solids* (McGraw-Hill, New York, 1963), Vol. 1, Chap. 1, p. 18.
- <sup>12</sup>W. L. Walters, D. G. Costello, J. G. Skrofonick, D. W. Palmer, W. E. Kane, and R. G. Herb, *Phys. Rev.* **125**, 2012 (1962).
- <sup>13</sup>A. F. Lifschitz and N. R. Arista, *Phys. Rev. A* **57**, 200 (1998).
- <sup>14</sup>I. Abril, R. Garcia-Molina, C. D. Denton, F. J. Pérez-Pérez, and N. R. Arista, *Phys. Rev. A* **58**, 357 (1998); C. D. Denton (private communication).
- <sup>15</sup>Z. Vager, D. S. Gemmell, and B. J. Zabransky, *Phys. Rev. A* **14**, 638 (1976).
- <sup>16</sup>P. L. Grande and G. Schiwietz, *Nucl. Instrum. Methods Phys. Res. B* **153**, 1 (1999).